Immunity, Volume *53*

Supplemental Information

Longitudinal Multi-omics Analyses Identify Responses of Megakaryocytes, Erythroid Cells, and Plasmablasts as Hallmarks of Severe COVID-19

Joana P. Bernardes, Neha Mishra, Florian Tran, Thomas Bahmer, Lena Best, Johanna I. Blase, Dora Bordoni, Jeanette Franzenburg, Ulf Geisen, Jonathan Josephs-Spaulding, Philipp Köhler, Axel Künstner, Elisa Rosati, Anna C. Aschenbrenner, Petra Bacher, Nathan Baran, Teide Boysen, Burkhard Brandt, Niklas Bruse, Jonathan Dörr, Andreas Dräger, Gunnar Elke, David Ellinghaus, Julia Fischer, Michael Forster, Andre Franke, Sören Franzenburg, Norbert Frey, Anette Friedrichs, Janina Fuß, Andreas Glück, Jacob Hamm, Finn Hinrichsen, Marc P. Hoeppner, Simon Imm, Ralf Junker, Sina Kaiser, Ying H. Kan, Rainer Knoll, Christoph Lange, Georg Laue, Clemens Lier, Matthias Lindner, Georgios Marinos, Robert Markewitz, Jacob Nattermann, Rainer Noth, Peter Pickkers, Klaus F. Rabe, Alina Renz, Christoph Röcken, Jan Rupp, Annika Schaffarzyk, Alexander Scheffold, Jonas Schulte-Schrepping, Domagoj Schunk, Dirk Skowasch, Thomas Ulas, Klaus-Peter Wandinger, Michael Wittig, Johannes Zimmermann, Hauke Busch, Bimba F. Hoyer, Christoph Kaleta, Jan Heyckendorf, Matthijs Kox, Jan Rybniker, Stefan Schreiber, Joachim L. Schultze, Philip Rosenstiel, HCA Lung Biological Network, and the Deutsche COVID-19 Omics Initiative (DeCOI)

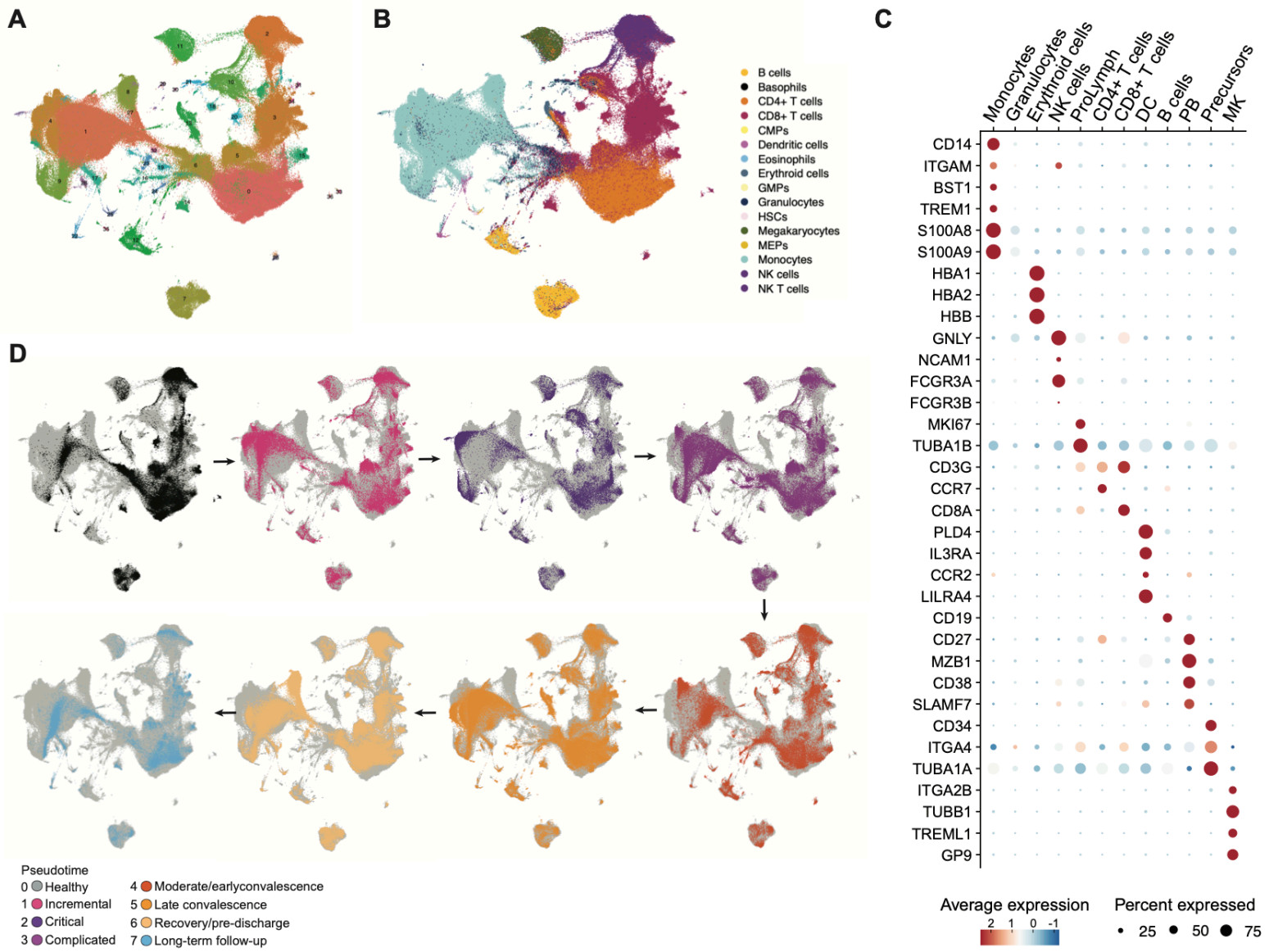
A
B
B cells
Basophils
CD4+ T cells
CD8+ T cells
CMPs
Dendritic cells
Eosinophils
Erythroid cells
GMPs
Granulocytes
HSCs
Megakaryocytes
MEPs
Monocytes
NK cells
NK T cells
C
Monocytes
Granulocytes
Erythroid cells
NK cells
ProLymph
CD4+ T cells
CD8+ T cells
DC
B cells
PB
Precursors
MK
CD14
ITGAM
BST1
TREM1
S100A8
S100A9
HBA1
HBA2
HBB
GNLY
NCAM1
FCGR3A
FCGR3B
MKI67
TUBA1B
CD3G
CCR7
CD8A
PLD4
IL3RA
CCR2
LILRA4
CD19
CD27
MZB1
CD38
SLAMF7
CD34
ITGA4
TUBA1A
ITGA2B
TUBB1
TREML1
GP9
Average expression
2 1 0 -1
Percent expressed
25 50 75
D
Pseudotime
0 Healthy
1 Incremental
2 Critical
3 Complicated
4 Moderate/earlyconvalescence
5 Late convalescence
6 Recovery/pre-discharge
7 Long-term follow-up

E

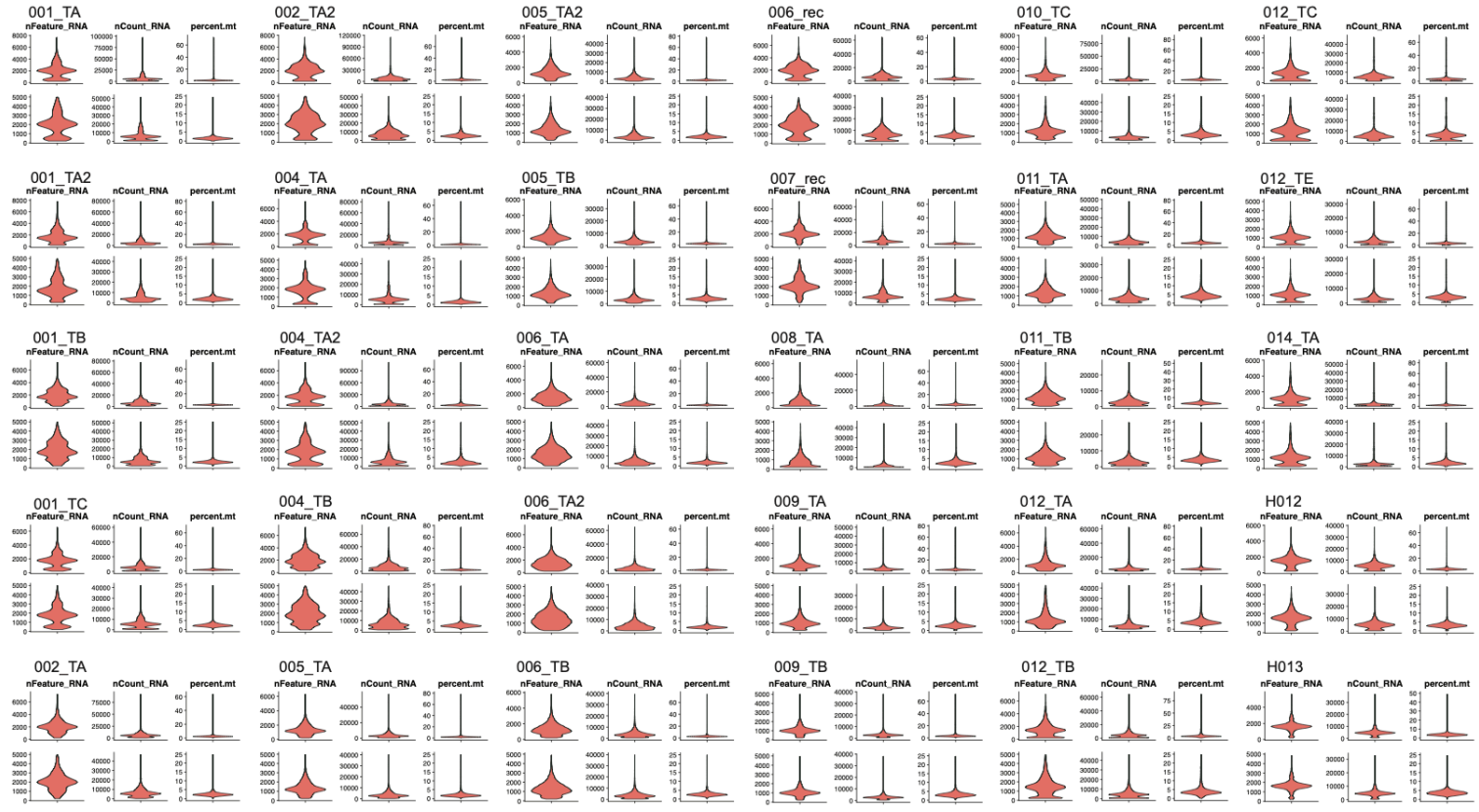
001_TA
002_TA2
005_TA2
006_rec
010_TC
012_TC
001_TA2
004_TA
005_TB
007_rec
011_TA
012_TE
001_TB
004_TA2
006_TA
008_TA
011_TB
014_TA
001_TC
004_TB
006_TA2
009_TA
012_TA
H012
002_TA
005_TA
006_TB
009_TB
012_TB
H013
nFeature_RNA
nCount_RNA
percent.mt

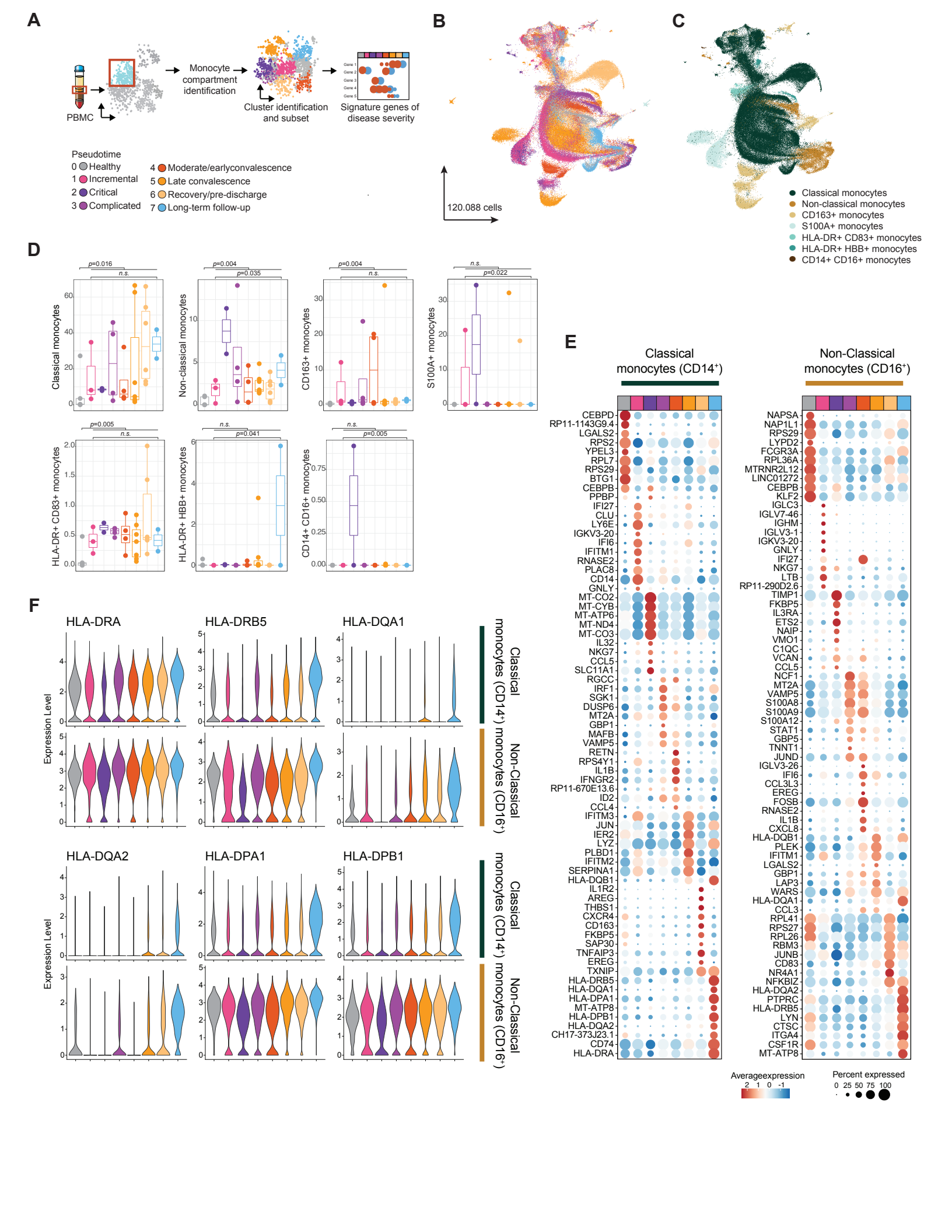
A
PBMC
Monocyte compartment identification
Cluster identification and subset
Signature genes of disease severity
Pseudotime
0 Healthy
1 Incremental
2 Critical
3 Complicated
4 Moderate/earlyconvalescence
5 Late convalescence
6 Recovery/pre-discharge
7 Long-term follow-up
B
120.088 cells
C
Classical monocytes
Non-classical monocytes
CD163+ monocytes
S100A+ monocytes
HLA-DR+ CD83+ monocytes
HLA-DR+ HBB+ monocytes
CD14+ CD16+ monocytes
D
Classical monocytes
Non-classical monocytes
CD163+ monocytes
S100A+ monocytes
HLA-DR+ CD83+ monocytes
HLA-DR+ HBB+ monocytes
CD14+ CD16+ monocytes
p=0.016
n.s.
p=0.004
p=0.035
p=0.004
n.s.
n.s.
p=0.022
p=0.005
n.s.
n.s.
p=0.041
n.s.
p=0.005
E
Classical monocytes (CD14+)
Non-Classical monocytes (CD16+)
CEBPD
RP11-1143G9.4
LGALS2
RPS2
YPEL3
RPL7
RPS29
BTG1
CEBPB
PPBP
IFI27
CLU
LY6E
IGKV3-20
IFI6
IFITM1
RNASE2
PLAC8
CD14
GNLY
MT-CO2
MT-CYB
MT-ATP6
MT-ND4
MT-CO3
IL32
NKG7
CCL5
SLC11A1
RGCC
IRF1
SGK1
DUSP6
MT2A
GBP1
MAFB
VAMP5
RETN
RPS4Y1
IL1B
IFNGR2
RP11-670E13.6
ID2
CCL4
IFITM3
JUN
IER2
LYZ
PLBD1
IFITM2
SERPINA1
HLA-DQB1
IL1R2
AREG
THBS1
CXCR4
CD163
FKBP5
SAP30
TNFAIP3
EREG
TXNIP
HLA-DRB5
HLA-DQA1
HLA-DPA1
MT-ATP8
HLA-DPB1
HLA-DQA2
CH17-373J23.1
CD74
HLA-DRA
NAPSA
NAP1L1
RPS29
LYPD2
FCGR3A
RPL36A
MTRNR2L12
LINC01272
CEBPB
KLF2
IGLC3
IGLV7-46
IGHM
IGLV3-1
IGKV3-20
GNLY
IFI27
NKG7
LTB
RP11-290D2.6
TIMP1
FKBP5
IL3RA
ETS2
NAIP
VMO1
C1QC
VCAN
CCL5
NCF1
MT2A
VAMP5
S100A8
S100A9
S100A12
STAT1
GBP5
TNNT1
JUND
IGLV3-26
IFI6
CCL3L3
EREG
FOSB
RNASE2
IL1B
CXCL8
HLA-DQB1
PLEK
IFITM1
LGALS2
GBP1
LAP3
WARS
HLA-DQA1
CCL3
RPL41
RPS27
RPL26
RBM3
JUNB
CD83
NR4A1
NFKBIZ
HLA-DQA2
PTPRC
HLA-DRB5
LYN
CTSC
ITGA4
CSF1R
MT-ATP8
Averageexpression
2 1 0 -1
Percent expressed
0 25 50 75 100
F
HLA-DRA
HLA-DRB5
HLA-DQA1
HLA-DQA2
HLA-DPA1
HLA-DPB1
Expression Level
Classical monocytes (CD14+)
Non-Classical monocytes (CD16+)

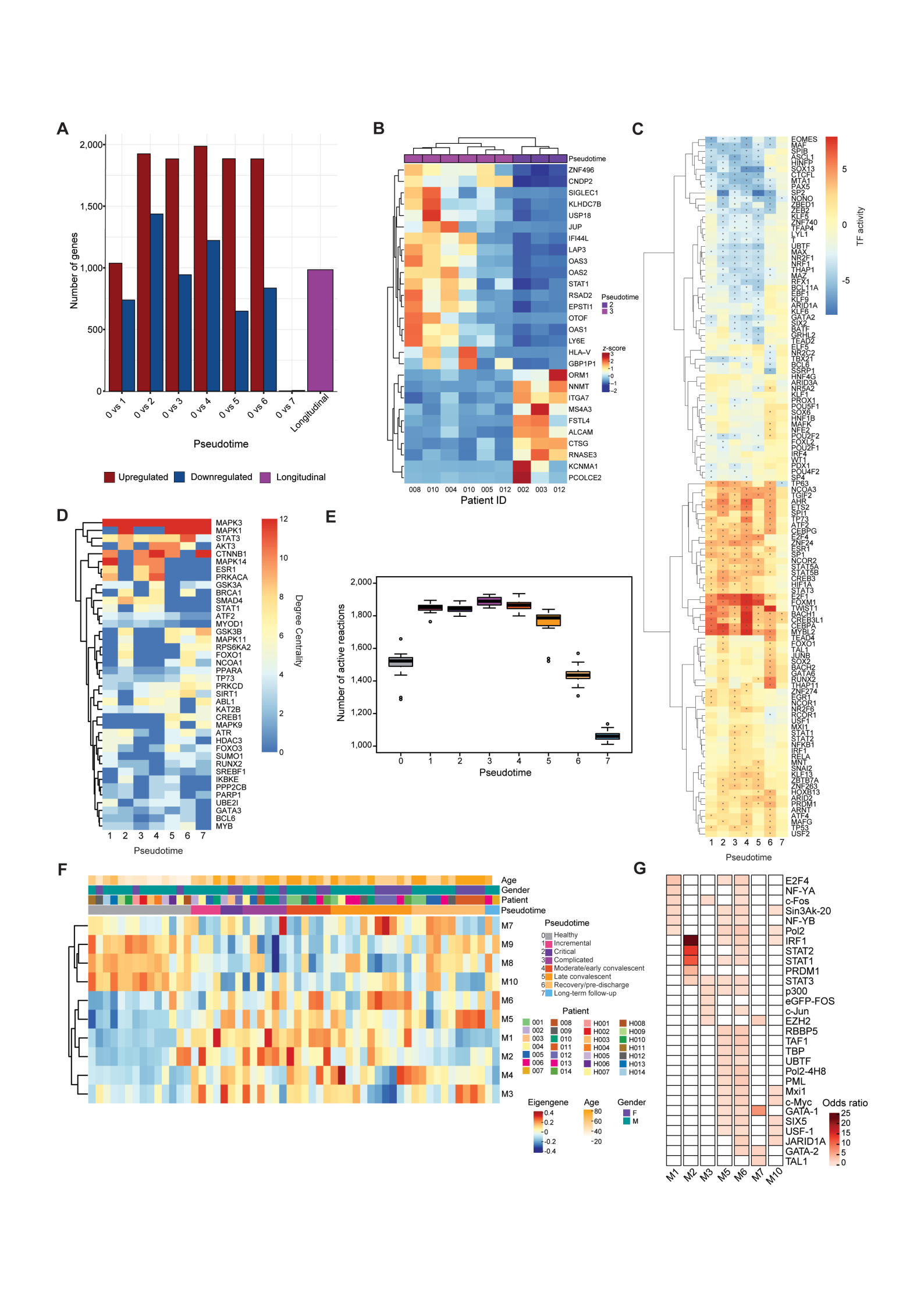
A
Number of genes
2,000
1,500
1,000
500
0
0 vs 1
0 vs 2
0 vs 3
0 vs 4
0 vs 5
0 vs 6
0 vs 7
Longitudinal
Pseudotime
Upregulated
Downregulated
Longitudinal
B
Pseudotime
ZNF496
CNDP2
SIGLEC1
KLHDC7B
USP18
JUP
IFI44L
LAP3
OAS3
OAS2
STAT1
RSAD2
EPSTI1
OTOF
OAS1
LY6E
HLA–V
GBP1P1
ORM1
NNMT
ITGA7
MS4A3
FSTL4
ALCAM
CTSG
RNASE3
KCNMA1
PCOLCE2
Pseudotime
2
3
z-score
3
2
1
0
−1
−2
008 010 004 010 005 012 002 003 012
Patient ID
C
EOMES
MAF
SPIB
ASCL1
HINFP
SOX13
CTCFL
MTA1
PAX5
SP2
NONO
ZBED1
ZEB2
KLF5
ZNF740
TFAP4
LYL1
T
UBTF
MAX
NR2F1
NRF1
THAP1
MAZ
RFX1
BCL11A
EBF1
KLF9
ARID1A
KLF6
GATA2
SIX2
BATF
GRHL2
TEAD2
ELF5
NR2C2
TBX21
BCL6
SSRP1
HNF4G
ARID3A
NR5A2
KLF1
PROX1
POU5F1
SOX6
HNF1B
MAFK
NFE2
POU2F2
FOXL2
POU2F1
IRF4
WT1
PDX1
POU4F2
SP4
TP63
NCOA3
TGIF2
AHR
ETS2
SPI1
TP73
ATF2
CEBPG
E2F4
ZNF24
ESR1
SP1
NCOR2
STAT5A
STAT5B
CREB3
HIF1A
STAT3
E2F1
FOXM1
TWIST1
BACH1
CREB3L1
CEBPA
MYBL2
TEAD4
FOXO1
TAL1
JUNB
SOX2
BACH2
GATA6
RUNX2
THAP11
ZNF274
EGR1
NCOR1
NR2F6
RCOR1
USF1
MXI1
STAT1
STAT2
NFKB1
IRF1
RELA
MNT
SNAI2
KLF13
ZBTB7A
ZNF263
HOXB13
ARID2
PRDM1
ARNT
ATF4
MAFG
TP53
USF2
5
0
-5
TF activity
1 2 3 4 5 6 7
Pseudotime
D
MAPK3
MAPK1
STAT3
AKT3
CTNNB1
MAPK14
ESR1
PRKACA
GSK3A
BRCA1
SMAD4
STAT1
ATF2
MYOD1
GSK3B
MAPK11
RPS6KA2
FOXO1
NCOA1
PPARA
TP73
PRKCD
SIRT1
ABL1
KAT2B
CREB1
MAPK9
ATR
HDAC3
FOXO3
SUMO1
RUNX2
SREBF1
IKBKE
PPP2CB
PARP1
UBE2I
GATA3
BCL6
MYB
12
10
8
6
4
2
0
Degree Centrality
1 2 3 4 5 6 7
Pseudotime
E
Number of active reactions
2,000
1,800
1,600
1,400
1,200
1,000
0 1 2 3 4 5 6 7
Pseudotime
F
Age
Gender
Patient
Pseudotime
M7
M9
M8
M10
M6
M5
M1
M2
M4
M3
Pseudotime
0 Healthy
1 Incremental
2 Critical
3 Complicated
4 Moderate/early convalescent
5 Late convalescent
6 Recovery/pre-discharge
7 Long-term follow-up
Patient
001 002 003 004 005 006 007
008 009 010 011 012 013 014
H001 H002 H003 H004 H005 H006 H007
H008 H009 H010 H011 H012 H013 H014
Eigengene
0.4
0.2
0
-0.2
-0.4
Age
80
60
40
20
Gender
F
M
G
E2F4
NF-YA
c-Fos
Sin3Ak-20
NF-YB
Pol2
IRF1
STAT2
STAT1
PRDM1
STAT3
p300
eGFP-FOS
c-Jun
EZH2
RBBP5
TAF1
TBP
UBTF
Pol2-4H8
PML
Mxi1
c-Myc
GATA-1
SIX5
USF-1
JARID1A
GATA-2
TAL1
Odds ratio
25
20
15
10
5
0
M1 M2 M3 M5 M6 M7 M10

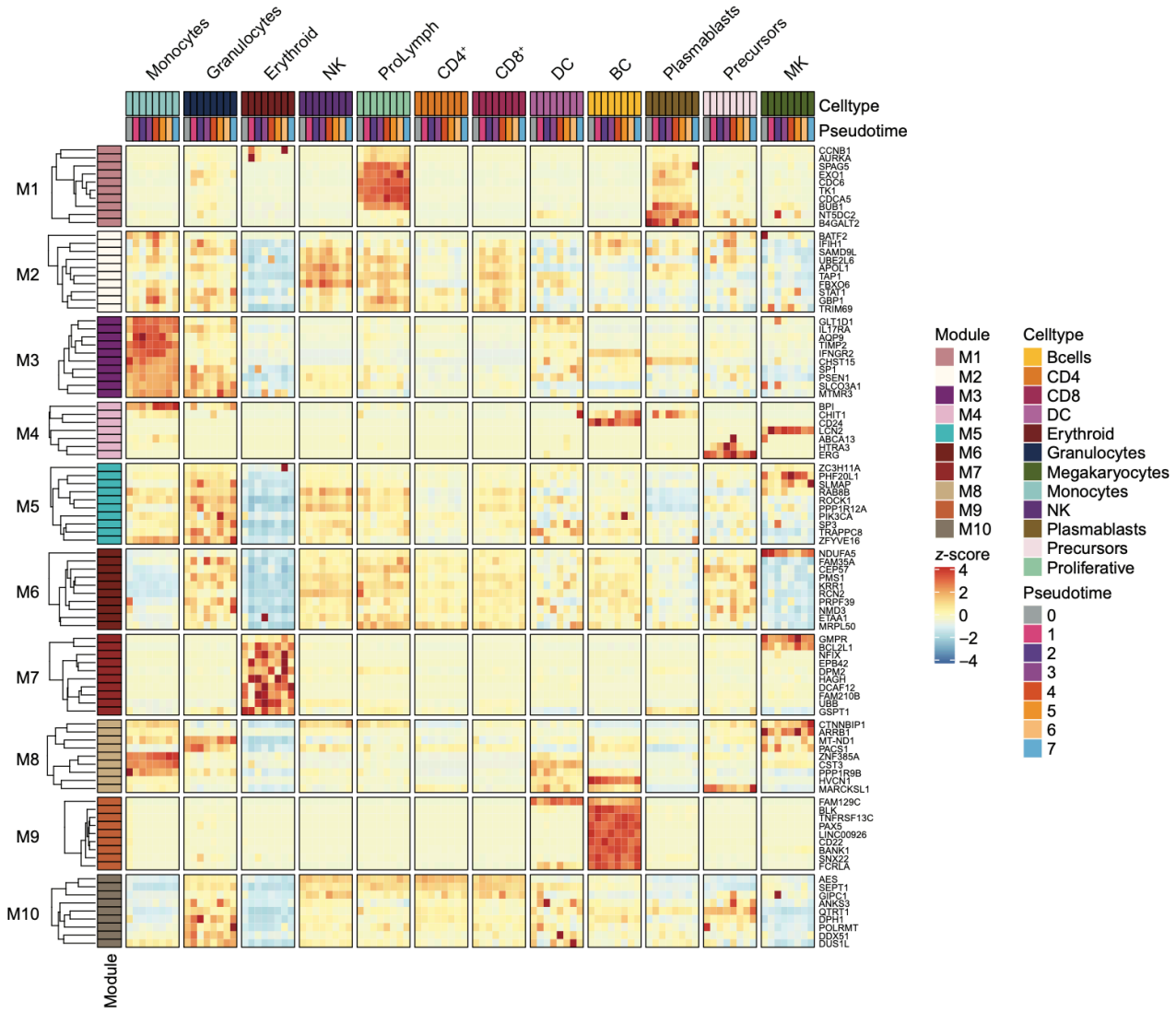
Monocytes
Granulocytes
Erythroid
NK
ProLymph
CD4+
CD8+
DC
BC
Plasmablasts
Precursors
MK
Celltype
Pseudotime
M1
M2
M3
M4
M5
M6
M7
M8
M9
M10
Module
CCNB1
AURKA
SPAG5
EXO1
CDC6
TK1
CDCA5
BUB1
NT5DC2
B4GALT2
BATF2
IFIH1
SAMD9L
UBE2L6
APOL1
TAP1
FBXO6
STAT1
GBP1
TRIM69
GLT1D1
IL7RA
AQP9
TIMP2
IFNGR2
CHST15
SPT
PSEN1
SLCO3A1
MTMR3
BPI
CHIT1
CD24
LCN2
ABCA13
HTRA3
ERG
ZC3H11A
PHF20L1
SLMAP
RAB8B
ROCK1
PPP1R12A
PIK3CA
SPZ
TRAPPC8
ZFYVE16
NDUFA5
FAM59A
CEP57
PMS1
KRR1
RCN2
PRPF39
NMD3
ETAA1
MRPL50
GMPR
BCL2L1
NFIX
EPB42
DPM2
HAGH
DCAF12
FAM210B
UBB
GSPT1
CTNNBIP1
ARRB1
MT-ND1
PACS1
ZNF385A
CST3
PPP1R9B
HVCN1
MARCKSL1
FAM129C
BLK
TNFRSF13C
PAX5
LINC00926
CD22
BANK1
SNX22
FCRLA
AES
SEPT1
GIPC1
ANKS3
QTRT1
DPH1
POLRMT
DDX51
DUS1L
Module
M1
M2
M3
M4
M5
M6
M7
M8
M9
M10
z-score
4
2
0
−2
−4
Celltype
Bcells
CD4
CD8
DC
Erythroid
Granulocytes
Megakaryocytes
Monocytes
NK
Plasmablasts
Precursors
Proliferative
Pseudotime
0
1
2
3
4
5
6
7

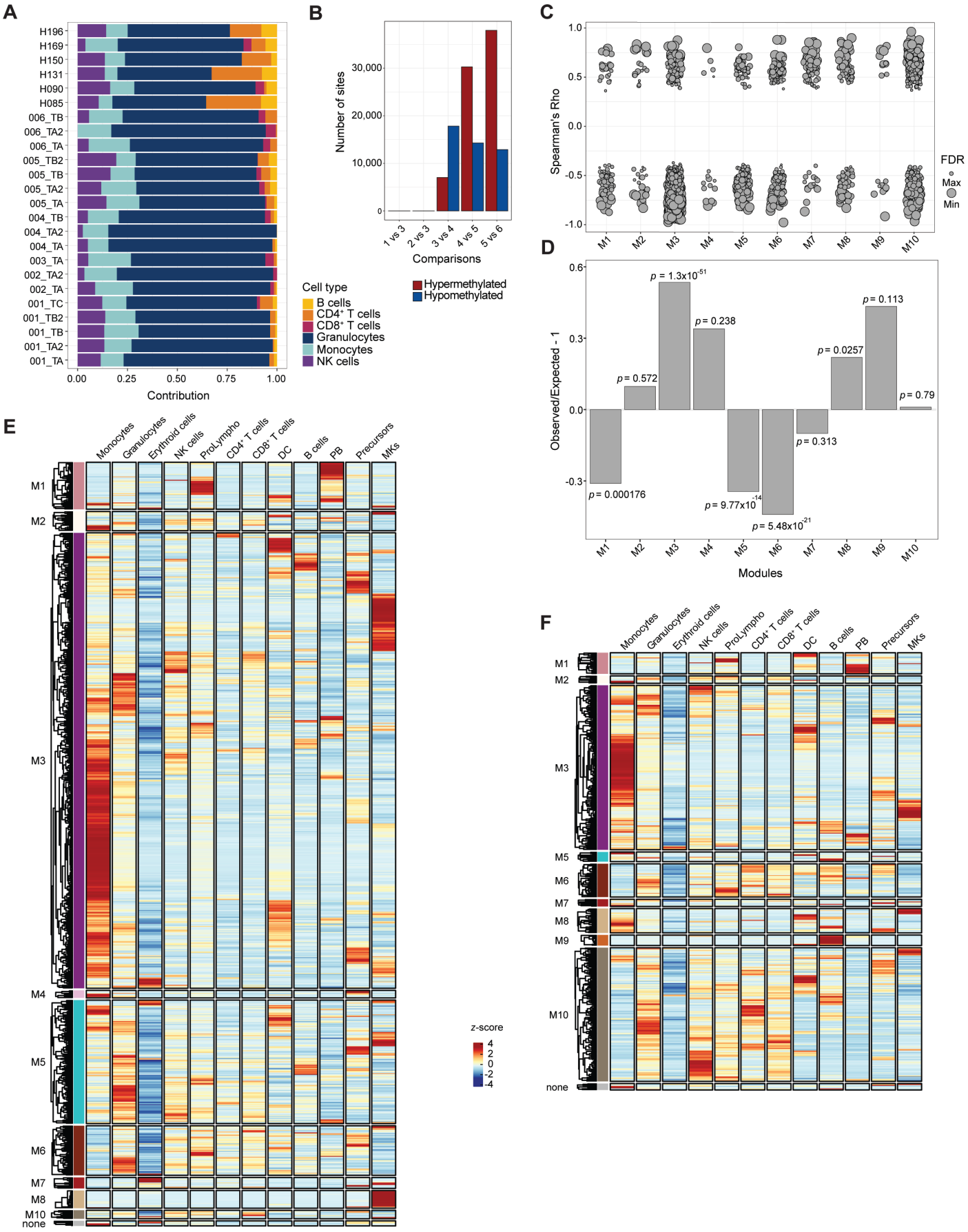
A
H196
H169
H150
H131
H090
H085
006_TB
006_TA2
006_TA
005_TB2
005_TB
005_TA2
005_TA
004_TB
004_TA2
004_TA
003_TA
002_TA2
002_TA
001_TC
001_TB2
001_TB
001_TA2
001_TA
0.00
0.25
0.50
0.75
1.00
Contribution
B
Number of sites
30,000
20,000
10,000
0
1 vs 3
2 vs 3
3 vs 4
4 vs 5
5 vs 6
Comparisons
Hypermethylated
Hypomethylated
Cell type
B cells
CD4+ T cells
CD8+ T cells
Granulocytes
Monocytes
NK cells
C
Spearman's Rho
1.0
0.5
0.0
-0.5
-1.0
FDR
Max
Min
M1
M2
M3
M4
M5
M6
M7
M8
M9
M10
D
Observed/Expected - 1
0.6
0.3
0.0
-0.3
p = 1.3x10-51
p = 0.238
p = 0.572
p = 0.0257
p = 0.113
p = 0.79
p = 0.313
p = 0.000176
p = 9.77x10-14
p = 5.48x10-21
Modules
E
Monocytes
Granulocytes
Erythroid cells
NK cells
ProLympho
CD4+ T cells
CD8+ T cells
DC
B cells
PB
Precursors
MKs
M1
M2
M3
M4
M5
M6
M7
M8
M10
none
z-score
4
2
0
-2
-4
F
Monocytes
Granulocytes
Erythroid cells
NK cells
ProLympho
CD4+ T cells
CD8+ T cells
DC
B cells
PB
Precursors
MKs
M1
M2
M3
M5
M6
M7
M8
M9
M10
none

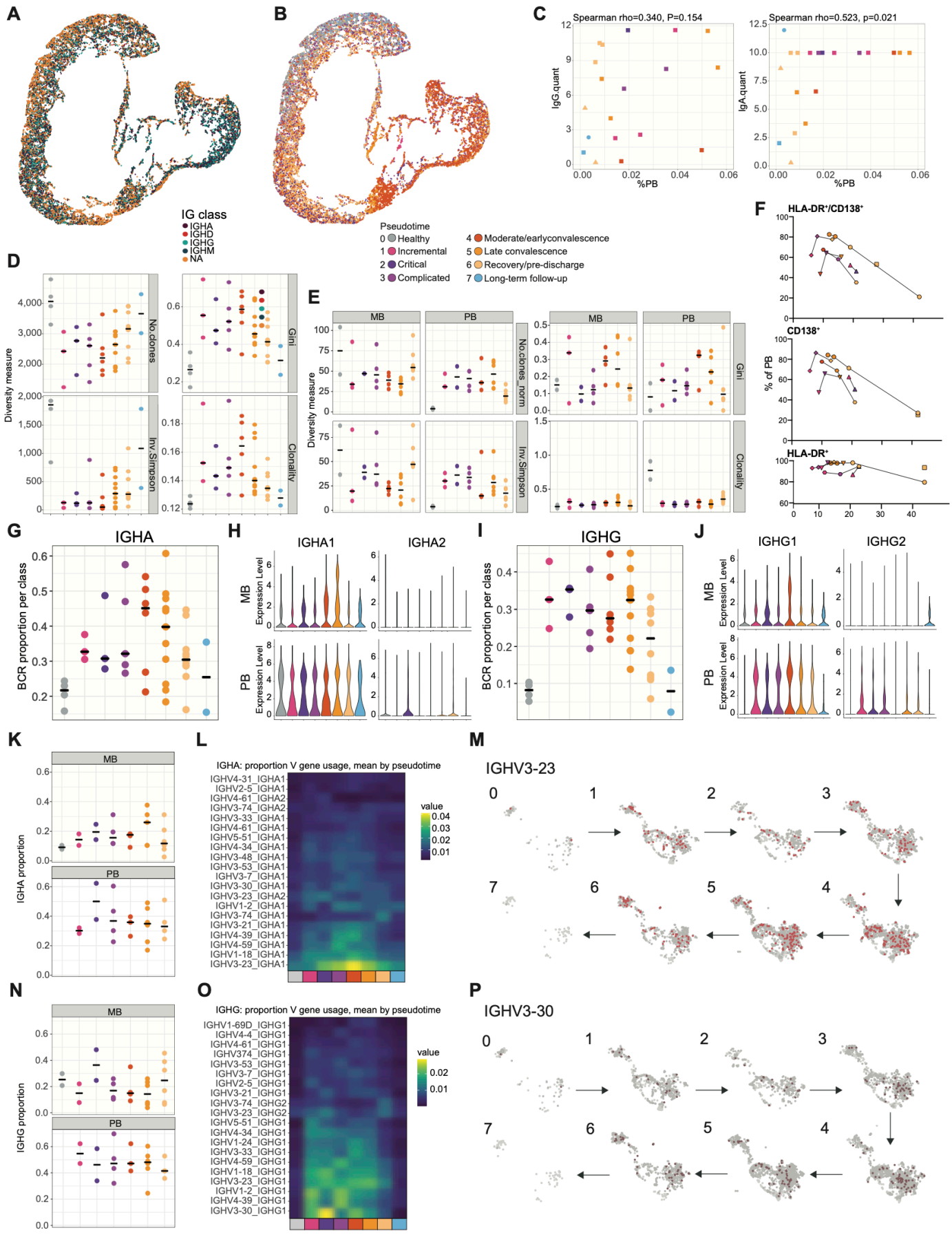
A
B
C
Spearman rho=0.340, P=0.154
Spearman rho=0.523, p=0.021
IgG.quant
IgA.quant
%PB
IG class
IGHA
IGHD
IGHG
IGHM
NA
Pseudotime
0 Healthy
1 Incremental
2 Critical
3 Complicated
4 Moderate/earlyconvalescence
5 Late convalescence
6 Recovery/pre-discharge
7 Long-term follow-up
D
Diversity measure
No.clones
Gini
Inv.Simpson
Clonality
E
MB
PB
No.clones_norm
F
HLA-DR+/CD138+
CD138+
HLA-DR+
% of PB
G
IGHA
BCR proportion per class
H
IGHA1
IGHA2
Expression Level
I
IGHG
J
IGHG1
IGHG2
K
IGHA proportion
L
IGHA: proportion V gene usage, mean by pseudotime
value
IGHV4-31_IGHA1
IGHV2-5_IGHA1
IGHV4-61_IGHA2
IGHV3-74_IGHA2
IGHV3-33_IGHA1
IGHV4-61_IGHA1
IGHV5-51_IGHA1
IGHV4-34_IGHA1
IGHV3-48_IGHA1
IGHV3-53_IGHA1
IGHV3-7_IGHA1
IGHV3-30_IGHA1
IGHV3-23_IGHA2
IGHV1-2_IGHA1
IGHV3-74_IGHA1
IGHV3-21_IGHA1
IGHV4-39_IGHA1
IGHV4-59_IGHA1
IGHV1-18_IGHA1
IGHV3-23_IGHA1
M
IGHV3-23
N
IGHG proportion
O
IGHG: proportion V gene usage, mean by pseudotime
IGHV1-69D_IGHG1
IGHV4-4_IGHG1
IGHV4-61_IGHG1
IGHV374_IGHG1
IGHV3-53_IGHG1
IGHV3-7_IGHG1
IGHV2-5_IGHG1
IGHV3-21_IGHG1
IGHV3-74_IGHG2
IGHV3-23_IGHG2
IGHV5-51_IGHG1
IGHV4-34_IGHG1
IGHV1-24_IGHG1
IGHV3-33_IGHG1
IGHV4-59_IGHG1
IGHV1-18_IGHG1
IGHV3-23_IGHG1
IGHV1-2_IGHG1
IGHV4-39_IGHG1
IGHV3-30_IGHG1
P
IGHV3-30

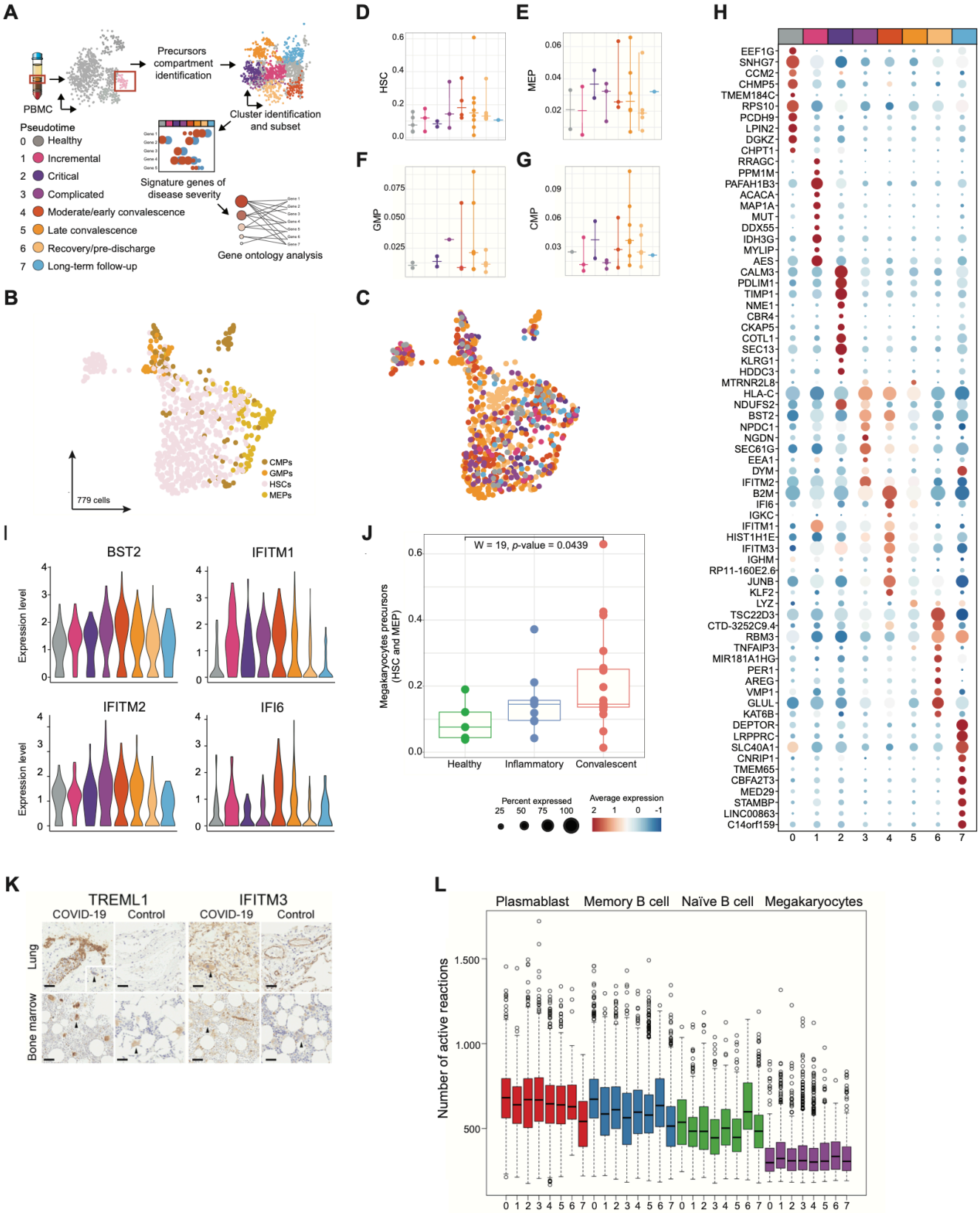
A
PBMC
Precursors compartment identification
Cluster identification and subset
Signature genes of disease severity
Gene ontology analysis
Pseudotime
0 Healthy
1 Incremental
2 Critical
3 Complicated
4 Moderate/early convalescence
5 Late convalescence
6 Recovery/pre-discharge
7 Long-term follow-up
B
779 cells
CMPs
GMPs
HSCs
MEPs
C
D
HSC
E
MEP
F
GMP
G
CMP
H
EEF1G
SNHG7
CCM2
CHMP5
TMEM184C
RPS10
PCDH9
LPIN2
DGKZ
CHPT1
RRAGC
PPM1M
PAFAH1B3
ACACA
MAP1A
MUT
DDX55
IDH3G
MYLIP
AES
CALM3
PDLIM1
TIMP1
NME1
CBR4
CKAP5
COTL1
SEC13
KLRG1
HDDC3
MTRNR2L8
HLA-C
NDUFS2
BST2
NPDC1
NGDN
SEC61G
EEA1
DYM
IFITM2
B2M
IFI6
IGKC
IFITM1
HIST1H1E
IFITM3
IGHM
RP11-160E2.6
JUNB
KLF2
LYZ
TSC22D3
CTD-3252C9.4
RBM3
TNFAIP3
MIR181A1HG
PER1
AREG
VMP1
GLUL
KAT6B
DEPTOR
LRPPRC
SLC40A1
CNRIP1
TMEM65
CBFA2T3
MED29
STAMBP
LINC00863
C14orf159
0 1 2 3 4 5 6 7
I
BST2
IFITM1
IFITM2
IFI6
Expression level
J
W = 19, p-value = 0.0439
Megakaryocytes precursors (HSC and MEP)
Healthy
Inflammatory
Convalescent
Percent expressed
25 50 75 100
Average expression
2 1 0 -1
K
TREML1
IFITM3
COVID-19
Control
Lung
Bone marrow
L
Plasmablast
Memory B cell
Naïve B cell
Megakaryocytes
Number of active reactions
1.500
1.000
500
0 1 2 3 4 5 6 7 0 1 2 3 4 5 6 7 0 1 2 3 4 5 6 7 0 1 2 3 4 5 6 7

Table S2. Pseudotime definition. (related to Figure 1)

Pseudotime	Disease Phase	Clinical Score
0	Uninfected (Control)	1
1	Incremental	Increasing
2	Critical	9* - 13
3	Complicated	7 - 9*
4	Complicated	6
5	Moderate/early convalescence	4 - 5
6	Late convalescence	3
7	Long-term follow-up	1 - 2

The Clinical Score is composed by the sum of the WHO Ordinal Scale and three lab value-based subscores: CRP (0 p: < 30 mg/l, 1 p: ≥ 30 mg/l, 2 p: ≥ 100 mg/l, 3 p: ≥ 200 mg/l), IL-6 (0 p: < 200 ng/l, 1 p: ≥ 200 ng/l), ferritin (0 p: < 1000 mg/l, 1 p: ≥ 1000 mg/l, 2 p: ≥ 4000 mg/l).

* If Ordinal Scale is 6 p or higher, the disease phase was classified as "critical".

Table S4. Cohort 3 basic characteristics. (related to Figure 8)

Patient ID	Age	Sex	Death
COR005	67	F	no
COR010	73	M	**yes**
COR011	81	M	**yes**
COR012	73	M	**yes**
COR013	68	M	no
COR014	47	M	no
COR015	72	M	no
COR016	71	M	no
COR017	65	M	no
COR018	60	F	no
COR019	74	M	no
COR021	73	M	no
COR022	69	M	no
COR025	67	F	**yes**
COR026	70	F	no
COR027	68	M	no
COR028	60	F	no
COR031	74	M	no
COR032	53	M	no
COR033	61	M	no
COR035	57	M	no
COR037	54	F	no
COR039	64	M	no
COR041	62	M	no
COR042	64	M	no
COR043	76	M	no
COR045	60	M	**yes**
COR046	47	F	no
COR048	67	F	no
COR050	73	M	no
COR053	72	M	no
COR054	59	M	no
COR055	76	M	**yes**
COR056	65	F	no
COR057	69	M	**yes**
COR059	55	M	no
COR060	59	M	no
COR062	69	F	no
COR066	54	M	no
COR067	21	M	no

Abbreviations: F = female, M = male

Figure S1. Details of scRNA-seq (related to Figure 2)

A, Cluster UMAP representation of all merged samples. In total, 358.930 cells are depicted. Cells are coloured by Single R qualification.

B, SingleR UMAP representation of all merged samples. In total, 358.930 cells are depicted. Cells are coloured by cluster.

C, Dot plot for expression of cell type marker genes. Colour discriminates genes with increased (red) or decreased (blue) expression, while point sizes represents the number of cells per group expressing the corresponding gene.

D, Cells attributed to disease trajectory of COVID-19. For each UMAP, pseudotime-specific cells were highlighted by colour.

E, Quality control violin plots of individual samples. Up panel referring to cells before quality filtering based on percentage of mitochondria and bottom panels referring to filtered cells that were further use in the analysis.

Figure S2. Monocyte lineage patterns in COVID-19 (related to Figure 2)

A, Schematic workflow of the scRNA-seq analyses performed on monocytes identified in Figure 2.

B, Monocytes pseudotimes represented as a UMAP. In total 120.088 cells are depicted.

C, Monocytes represented as a UMAP. In total 120.088 cells are depicted. Clusters represented are classical monocytes (dark green), nonclassical monocytes (brown), $CD163^{+}$ monocytes (cream), $S100A^{+}$ monocytes (light blue), HLA-DR+ $CD83^{+}$ monocytes (blue), $HLA\text{-}DR^{+}$ HBB^{+} monocytes (dark blue) and $CD14^{+}CD16^{+}$ monocytes (dark brown).

D, Monocytes subtypes proportions grouped by disease phases. Points represent individual samples and horizontal bars the mean of a particular pseudotime. Pseudotimes are represented by colours.

E, Dot plot for signature genes in monocyte subtypes. Left panel depicting top signature genes per pseudotime of classical monocytes and right panel depicting top signature genes per pseudotime of nonclassical monocytes. Genes were selected based on increased expression of the ten most characteristic genes. Colour discriminates genes with increased (red) or decreased (blue) expression, while point sizes represents the number of cells per group expressing the corresponding gene.

F, Gene expression of genes of interest along the disease axis. Violin plot based on pseudotime expressions classified by colour for *HLA* genes.

Figure S3. Analysis of bulk RNA-seq data (related to Figure 3 and Figure 4)

A, Number of significantly differentially expressed genes (DEGs) between controls and COVID-19 pseudotimes and number of longitudinal DEGs across different pseudotimes. Colours discriminate genes with increased (red) or decreased (blue) expression in COVID-19 samples compared to controls and longitudinal DEGs (purple).

B, Heatmap showing genes differentially expressed between critical (pseudotime 2) and complicated (pseudotime 3) disease. The normalized gene counts are scaled by row and row-wise *z*-scores are plotted in the heatmap.

C, Heatmap depicting the activity of top 50% most variable transcriptions factors (TFs) across the seven pseudotimes relative to the controls. A star within a cell denotes a significant (p-value < 0.05) activation or inhibition of the respective TF.

D, Heatmap depicting the degree centrality of all inferred networks across the pseudotimes. Rows have been clustered by complete linkage according to their Euclidian distance.

E, Disease-state specific total metabolic activity for bulk RNA-seq data showing the total number of active reactions for context-specific metabolic models.

F, Eigengene heatmap of co-expression modules constructed using all pairwise and longitudinal differentially expressed genes. Columns are ordered by pseudotimes and annotated by age, gender and patient IDs.

G, Heatmap showing the significant enrichment, quantified by odds ratio, of transcription factor binding sites (TFBS) in the gene co-expression modules. Selected top TFs are visualized.

Figure S4. Projection of modules in scRNA-seq data (related to Figure 4)

Heatmap showing the average expression of module hub genes in different cell types and pseudotimes of cohort 1 (from scRNA-seq data). Row-wise *z*-scores of the average gene counts are plotted in the heatmap. Genes are labelled by the co-expression modules and are hierarchically clustered for each module separately.

Figure S5. Genome-wide DNA methylation patterns in COVID-19 (related to Figure 4)

A, RnBeads computational deconvolution of whole blood samples from COVID-19 patients and controls based on EPIC array data.

B, Number of significantly differentially methylated positions (DMPs) between subsequent COVID-19 pseudotimes. Colours discriminate hypermethylated (red) and hypomethylated (blue) sites in later COVID-19 pseudotimes compared to former.

C, Correlation between co-expression module genes and their nearby DMPs. Each point represents a gene, and the size of the points is proportional to statistical significance (FDR) of the correlation with larger points being more significant. DMP-DEG correlations with FDR < 0.05 are

visualized. The positions of individual points are jittered horizontally in order to show the density of the data.

D, Over-representation and under-representation of significantly correlated DMP-DEG in each of the co-expression modules. The over-/under-representation is quantified as the ratio of observed and expected number of correlated genes present in each module under the Chi-square distribution.

E, Heatmap showing the average expression of canonical DMP-DEGs with increased expression in active disease (pseudotimes 1, 2, 3 and 4) in different cell-types of cohort 1 (from scRNA-seq data). The average expression in severe stages of the disease (pseudotimes 1, 2 and 3) is shown. The average genes counts are scaled by row and row-wise z-scores are plotted in the heatmap. Genes are labelled by the co-expression modules and are hierarchically clustered for each module separately.

F, Heatmap showing the average expression of canonical DMP-DEGs with decreased expression in disease recovery (pseudotimes 5 and 6) in different cell-types of cohort 1 (from scRNA-seq data). The average expression in recovery stages of the disease (pseudotimes 5 and 6) is shown. The average genes counts are scaled by row and row-wise z-scores are plotted in the heatmap. Genes are labelled by the co-expression modules and are hierarchically clustered for each module separately.

Figure S6. B cell lineage patterns and BCR changes in COVID-19 (related to Figure 5)

A, Cell trajectory analysis of B cell compartment. Cell trajectory was calculated using Monocle3 and the cells coloured by IG class. Pseudotimes are represented by colours. Spearman correlation values on top of each graph.

B, Cell trajectory analysis of B cell compartment. Cell trajectory was calculated using Monocle3 and the cells coloured by pseudotime.

C, Correlation of antibodies of interest with proportion of plasmablast. Left panel corresponds to IgG levels and right panel to IgA levels. Plasmablast levels as percentage to total cell numbers and Ig levels as OD measurements.

D, BCR diversity measures classified by pseudotime. Data based on bulk BCR-seq analysis. BCR diversity as number of clones (top left), inverse Simpson index (bottom left), Gini inequality index (top right) and clonality (bottom right).

E, BCR diversity measures for B cell subtypes classified by pseudotime. Data based on scBCR-seq. Diversity measures grouped by B cell subtypes memory B cells and plasmablasts. BCR diversity as number of clones (top left), inverse Simpson index (bottom left), Gini-Simpson index (top right) and clonality (bottom right).

F, Flow cytometry analysis of Plasmablasts. Plasmablasts were stained for HLA-DR and CD138. Double positive HLA-DR$^+$/CD138$^+$ cells on top panel, CD138$^+$ cells on center panel and HLA-DR$^+$ cells on bottom panel. Proportions of plasmablasts were plotted against the sampling time relative to the disease onset. The points were coloured by corresponding pseudotime and connected by patient. Only patients from Kiel cohort (*n* = 7 individuals) are depicted.

G, IGHA BCR proportion classified by pseudotime. Data based on bulk BCR-seq analysis.

H, Gene expression of genes related to IGHA by pseudotimes. *IGHA1* and *IGHA2* expression classified by pseudotimes (colour) for Memory B cells (top) or plasmablast (bottom).

I, IGHG BCR proportion classified by pseudotime. Data based on bulk BCR-seq analysis.

J, Gene expression of genes related to IGHG by pseudotimes. *IGHG1* and *IGHG2* expression classified by pseudotimes (colour) for Memory B cells (top) or plasmablast (bottom).

K, IGHA BCR proportion for B cell subtypes. Memory B cells on top and plasmablast on bottom classified by pseudotime. Data based on scBCR-seq analysis.

L, Heatmap for proportion of V usage of IGHA. Top genes related to IGHA1 or IGHA2 by pseudotime. Usage frequency depicted by colour intensity. Data based on bulk BCR-seq analysis.

M, IGHV3-23 expression in plasmablasts during disease trajectory. For each UMAP, IGHV3-23-expressing cells were highlighted (red).

N, IGHG BCR proportion for B cell subtypes. Memory B cells on top and plasmablast in bottom classified by pseudotime.

O, Heatmap for proportion of V usage of IGHG. Top genes related to IGHG1 or IGHG2 by pseudotime. Usage frequency depicted by colour intensity. Data based on bulk BCR analysis.

P, IGHV3-30 expression in plasmablasts during disease trajectory. For each UMAP, IGHV3-30-expressing cells were highlighted (dark red).

Figure S7. Cell precursors patterns in COVID-19 (related to Figure 6)

A, Schematic workflow of the scRNA-seq analyses performed on the cell precursors identified in Figure 2.

B, Cell precursors represented as a UMAP. In total 779 cells are depicted. Clusters represented are HSCs (pink), MEPs (yellow), CMPs (dark yellow) and GMPs (light orange).

C, Cell precursors pseudotimes represented as a UMAP. In total 779 cells are depicted.

D, HSCs-specific proportions grouped by disease phases. Points represent individual samples and horizontal bars the mean of a particular pseudotime. Pseudotimes are represented by colours.

E, MEPs-specific proportions by disease phases, pseudotimes are represented by colours.

F, GMPs-specific proportions grouped by disease phases. Points represent individual samples and horizontal bars the mean of a particular pseudotime. Pseudotimes are represented by colours.

G, CMPs-specific proportions grouped by disease phases. Points represent individual samples and horizontal bars the mean of a particular pseudotime. Pseudotimes are represented by colours.
H, Dot plot for signature genes in cell precursors. Genes were selected based on increased expression of the ten most characteristic genes. Colour discriminates genes with increased (red) or decreased (blue) expression, while point sizes represents the number of cells per group expressing the corresponding gene.
I, Gene expression of genes of interest along the disease axis. Violin plot based on pseudotime expressions classified by colour for *BST2*, *IFITM1*, *IFITM2* and *IFI6.*
J, HSCs and MEPs proportions grouped by disease state. Points depicting samples classified as healthy controls in green, as inflammatory stages (pseudotimes 1-3) in blue or as convalescent stages (pseudotimes 4-7) in red. Statistics based on Mann-Whitney U test.
K, Representative anti-TREML1- and anti-IFITM3-immunostaining of tissue specimens obtained from autopsy material from patient 002 and a gender- and age-matched patient (control). Note immunostaining of the megakaryocytes (arrow head) and particularly the presence of large numbers of TREML1-immunopositive platelets in the vessel lumina of the COVID-19 patient (left upper subpanel). Hematoxylin counterstain. Original magnifications: 400-fold.
L, Number of active reactions during disease course. Number of reactions calculated based on the metabolic model for plasmablasts (red), memory B cells (blue), naïve B cells (green) and megakaryocytes (purple). Number of active reactions corrected for cell number.